Celal Bayar University Journal of Science
Volume 22, Issue 2, 2026, p 284-294
Doi: 10.18466/cbayarfbe.1829844
Research Article

Celal Bayar University Journal of Science

Spatiotemporal EEG Dynamics Across Early and Late Preictal Periods in Pediatric Focal Epilepsy

Hasan Fehmi Özel[1*]

[1] Manisa Celal Bayar University, Vocational School of Healthy Services, Manisa, Türkiye
* fehmiozel@gmail.com
* Orcid No: 0000-0003-1676-0648

Received: November 25, 2025
Accepted: March 5, 2026
DOI: 10.18466/cbayarfbe.1829844

Abstract

Objective: This study aimed to quantify the temporal and spatial dynamics of preictal cortical networks in pediatric refractory focal epilepsy using scale-independent EEG measurements. **Method:** For this purpose, the preictal (−35 to −5 min), interictal, early preictal (−35 to −20 min), and late preictal (−20 to −5 min) periods were examined in long-term scalp EEG recordings from pediatric patients in the CHB–MIT database. For the selected segments, the detrended fluctuation analysis (DFA) scale exponent, median power frequency (MPF), and aperiodic 1/f exponent (β) were calculated using SpecParam/FOOOF and IRASA. The metrics were summarized on an individual basis and analyzed using two-way repeated measures ANOVA with Šídák-corrected post-hoc tests and topographic mapping. **Findings:** The preictal period was characterized by increased DFA-α and MPF in fronto-temporal regions compared to the interictal period; during the interictal period, MPF foci shifted to posterior areas. Aperiodic β values showed steepening in frontal regions during the preictal period and exhibited a posterior-temporal gradient during the interictal period. Critically, during the transition from the early to late preictal period, fronto-temporal DFA-α and MPF values decreased, accompanied by a posterior-to-anterior spread of aperiodic β steepening. **Conclusion:** These findings indicate that cortical networks experience a collapse in long-range temporal correlations and a reorganization of the aperiodic spectral structure as seizure onset approaches. The observed loss of complexity, spectral slowing, and frontal aperiodic steepening, occurring simultaneously, suggest a heterogeneous nature of the preictal process and highlight the potential of scale-independent metrics in monitoring seizure risk.

Keywords: Aperiodic 1/f activity, EEG dynamics, epilepsy, Long-range temporal correlations, Median power frequency, Preictal brain states, Seizure prediction

1. Introduction

Epilepsy is a chronic neurological disorder characterized by synchronization patterns that emerge in neural networks. The synchronous discharge of neuron groups on short time scales can disrupt complexity and lower the seizure threshold. Therefore, not only the seizure itself but also the preictal period is important from an electrophysiological perspective. Predicting epileptic seizures is valuable in terms of patient welfare and quality of life. Selecting the correct time windows for evaluating dynamic changes in brain electrical activity in the context of seizures is a critical research topic [1]. Determining these time windows is possible thanks to high-resolution electroencephalography (EEG) and metrics that can be generated from EEG. EEG directly reflects fundamental statistical properties of neuronal groups, such as excitation/inhibition (E/I) balance, spectral slope (1/f β), and fractal time correlations [2,3]. Changes in these properties produced by neural electrical activity in the pre-seizure period can be considered neurophysiological indicators of decreased neural network stability and complexity [4].

Recent studies have shown that, in addition to the frequency-based periodic components of EEG, the time-dependent scaling structure can also provide information about seizure dynamics [5,6]. These features are evaluated using the Detrended Fluctuation Analysis (DFA) method, which is used to determine long-range temporal correlations (LRTC) and fractal structure in neural signals [7]. DFA reveals the signal's level of self-similarity by calculating the slope coefficient (α) on the variance-frequency curve of the time series in the log-log

plane. Changes in the α coefficient provide information about long-range dependence in the signal and, consequently, about changes in the stability of the system [4,8]. Depending on the value of the scale exponent α, the signal can be in a state of anti-correlation ($\alpha < 0.5$), positive long-range correlation ($0.5 < \alpha < 1.0$), or strongly persistent ($\alpha > 1.0$). The anti-correlation state indicates that the signal responds in the opposite direction to its previous state and exhibits a noise-like structure. For EEG time series, this state may be an indicator of irregular neuronal activity and weakened network stability [7,9]. The physiological range where positive long-range correlations (persistent LRTC) are found produces a spectrum close to white noise at $\alpha \approx 0.5$ and close to 1/f pink noise at $\alpha \approx 1.0$. In healthy neurodynamic systems, α is generally in the range of 0.6–0.9 [4,7]. A shift of the DFA α coefficient away from the neurodynamic range indicates complexity loss and/or complexity collapse. The onset of increased synchronous activity in neuron groups and the approach to the epileptic seizure threshold can be detected by changes in the DFA α coefficient [6]. Therefore, the aperiodic component of the EEG can be evaluated using the DFA-α coefficient in the pre-seizure period. However, an increase in the spectral slope β value is associated with a relative gain in power of the slow frequency components and may indicate that cortical electrical activity is shifting towards greater synchrony and lower complexity [3,4]. Therefore, the combined evaluation of β (FOOOF and IRASA) parameters and the DFA-α coefficient allows for a comprehensive analysis of linear and fractal changes in pre-seizure network dynamics.

Recent studies have shown that there may be distinct differences in EEG dynamics exhibiting scaling between the early and late subphases of the preictal period [7,10]. It has been reported that DFA α values are closer to the neurodynamic norm range in early preictal phases and are markedly reduced in late preictal phases; this is associated with complexity loss and critical slowing phenomena in the system. Similarly, the steepening observed in the β slope during the late preictal phase may indicate an increased dependence on low-frequency (slow) activities and the predominance of intra-network inhibition [11]. Therefore, comparing electrophysiological changes between the early and late preictal periods is important for distinguishing the fractal and spectral transformations that epileptic networks undergo as they approach the critical threshold.

Loss of stability in cortical networks during the preictal period can be better characterized by a comprehensive analysis of long-range temporal correlations, spectral slowing, and changes in aperiodic (1/f) background activity, rather than by a single marker [12]. In this context, our study considers the preictal period not as a homogeneous whole but as a dynamic process involving early and late phases. Using the CHB-MIT Pediatric EEG database, interactions between DFA-α, aperiodic spectral slope β, and MPF were analyzed. Our primary aim is to determine the topological signature of scale-free complexity loss and spectral reorganization in cortical networks as they approach seizure onset by tracking the spatiotemporal course of these neurodynamic indicators.

2. Materials and Methods

2.1 Dataset and Participants

Analyses were performed using the CHB–MIT Scalp EEG Database, which contains long-term scalp EEG recordings from pediatric patients with intractable epilepsy [13,14]. The dataset contains a total of 23 recording sessions from 22 pediatric subjects (5 males, 17 females) aged 1.5–22 years, with all recordings obtained using a 256 Hz sampling rate, 16-bit resolution, and the CHB -MIT's standardized 10–20-based 23-channel bipolar montage. Seizure onset and offset times were obtained from the .seizure annotation files provided with the dataset. Since clinical and demographic information was anonymized in the database, the study is considered a secondary data analysis and does not require additional ethical committee approval. Individuals with at least three seizure recordings per patient were included ($n \geq 3$ seizures to ensure a within-patient comparison design). Data channel integrity, artifact load, and missing data rate were checked in all analyzed segments. Oculomotor, EMG, and high-amplitude saturation artifacts were marked by independent review and excluded from the relevant windows. The clean data rate was maintained at ≥95% per individual.

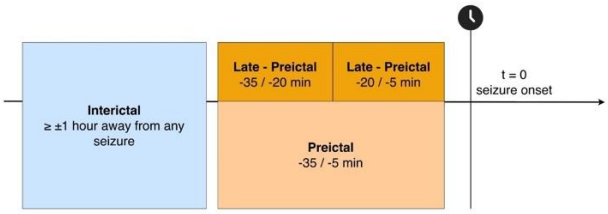

Figure 1. *Schematic representation of the temporal segmentation used in the analysis.*

The seizure prediction framework was configured according to the criteria of Seizure Prediction Horizon (SPH)=5 min and Seizure Occurrence Period (SOP)=30 min, as recommended in the current literature. Accordingly: the preictal period was defined as −35 to −5 minutes before seizure onset, early preictal as −35 to −20 minutes, and late preictal as −20 to −5 minutes. The interictal period was selected from the same patient, at least ±1 hour away from any seizure, artifact-free, and circadian-matched segments due to their known effects on aperiodic power [2,15]). Raw recordings were processed using MNE-Python [16]. 0.5–45 Hz band-pass finite impulse response (FIR) filter (linear-phase, firwin) and a 50 Hz notch filter were applied to all channels. To prevent distortion of the 1/f component due to excessive filter steepness, the filter order was limited using MNE's automatic minimum-ripple setting. All analyses were performed on the original bipolar montage.

2.2 Median Power Frequency (MPF)

MPF was calculated using the cumulative power distribution method to determine the frequency below which half of the spectral power resides. First, the power spectral density (PSD) was calculated using the Welch periodogram method. The Hamming window function and a 50% overlap ratio were used in the PSD calculation. The analysis was performed in the 0.5–45 Hz frequency range. To determine the MPF, the cumulative sum of the PSD values in the selected frequency range was calculated and normalized to the total power. The first frequency value at which the normalized cumulative power spectrum reached the 50% threshold was recorded as the MPF.

2.3 Detrended Fluctuation Analysis (DFA)

The **DFA** method, which measures the self-similarity behavior of the EEG signal according to time scales, was applied to quantify long-range temporal correlations (LRTC). The DFA algorithm was first defined by Peng et al. (1994). The method has since become the standard tool for LRTC analysis in EEG [7]. Calculations were performed on the band-limited Hilbert amplitude envelope (0.5–45 Hz) rather than on the raw fluctuation. This is because the literature clearly shows that DFA should measure the fractal structure derived from the underlying amplitude dynamics rather than the oscillatory component [8]. First, for each window, the time series was centered by subtracting the mean and then integrated:

$$y(i) = \sum_{k=1}^{i} (x(k) - \bar{x}) \qquad (2.1)$$

Then, 15 logarithmically equally spaced scales were determined in the range of 1–3 seconds (256–768 samples for 256 Hz sampling) to be compatible with the 60-second window length. For each scale, the integrated series was divided into consecutive segments of equal length, and detrending was performed using a first-order polynomial for each segment:

$$y(i) = a_n + b_n i \qquad (2.2)$$

Then, the second moment of the detrended deviations was calculated for each segment, and the fluctuation function for that scale was obtained as:

$$F(n) = \sqrt{\frac{1}{N_n}\sum_{k=1}^{N_n}\frac{1}{n}\sum_{i=1}^{n}\left[y(i+(k-1)n) - p_{n,k}(i)\right]^2} \qquad (2.3)$$

The obtained values were transferred to a log–log plane, and the DFA exponent (α) was calculated as the slope of the following linear regression:

$$\log F(n) = \alpha \log n + c \qquad (2.4)$$

This slope represents the scale-dependent correlation structure of the signal:
$\alpha \approx 0.5$ white noise,
$\alpha \approx 1.0$ pink noise (1/f),
$\alpha > 1.0$ strong positive long-range correlation
$\alpha < 0.5$ anti-correlation.
All DFA analyses were performed using Python (NumPy v1.26.0, SciPy v1.13.0).

2.4 Calculation of the Aperiodic (1/f) Spectral Component

The slope (β) of the aperiodic component of the EEG power spectrum was obtained using two independent methods: the parametric approach FOOOF/SpecParam [2] and the Irregular Resampling Auto-Spectral Analysis (IRASA) method [3]. Prior to applying both methods, the windowed power spectral density (PSD) estimate was calculated using the Welch periodogram (Hamming window, 50% overlap, 256 sample segment length). *SciPy signal.welch* (v1.13.0) was used for PSD calculations.
Separation of the Aperiodic Component with FOOOF/SpecParam: The FOOOF method is based on a parametric model that separates the EEG power spectrum into two components:

$$P(f) = L(f) + \sum_{k=1}^{K} G_k(f) \qquad (2.5)$$

where, represents the aperiodic component; represents the Gaussian-shaped oscillation peaks. The aperiodic component was modeled in the *"fixed"* mode without a knee term in the following linear log-log form:

$$L(f) = b - \beta \log(f) \qquad (2.6)$$

The frequency range was limited to 2–40 Hz. This range is where both the oscillatory and 1/f components are stably separated in pediatric EEG [2]. Peak width was constrained between 0.5–12 Hz, and a maximum of 10 peaks was allowed.

Separation of the Aperiodic Component with IRASA: IRASA isolates the aperiodic portion by suppressing the oscillatory component by taking the geometric mean of the oversampled and undersampled versions of the signal. According to the formulation given by Wen & Liu (2016). The data was resampled for each scaling factor h, the PSD was calculated for each level h, and the geometric mean of these two PSDs was taken to suppress the oscillatory component:

$$PSD_{\text{frac}}(f,h) = \sqrt{PSD(x_{h\uparrow}) \cdot PSD(x_{h\downarrow})} \qquad (2.7)$$

In this study, h was set to a total of 17 scaling coefficients between 1.1 and 1.9 in 0.05 increments, the PSDs obtained for each h were interpolated to the original frequency grid, and the median was taken for all h levels to obtain the pure aperiodic spectrum. The resulting aperiodic spectrum was transformed into log–log space in the 1–45 Hz range, and linear regression was applied:

$$\log P(f) = a - \beta_{\text{IRASA}} \log(f) \qquad (2.8)$$

The negative of the regression coefficient here was reported as β-IRASA. IRASA calculations were performed in a Python environment using SciPy (v1.13.0) and NumPy (v1.26) [17].
FOOOF is one of the first parametric methods that explicitly models periodic and aperiodic components and allows the 1/f variations in EEG to be related to physiological processes [2]. IRASA separates the spectrum into two independent components using a resampling-based decomposition and is effective in data with prominent oscillatory activity, such as EEG [3]. The combined use of the two methods in this study allowed for the verification of aperiodic slope changes in both a model-based (FOOOF) and model-independent (IRASA) manner.

2.5 Creation of Topological Maps

The topological distributions of the calculated parameters were generated by reprojecting the channel-specific features produced for EEG pairs recorded with bipolar montage onto the virtual electrode positions in the standard 10–20 system. First, a virtual electrode was created by assigning the relevant parameter value of each bipolar derivation to the geometric midpoint of two monopolar electrodes. Subsequently, all intermediate nodes were placed on a three-dimensional head model in standardized 10–20 coordinate space using the MNE-Python infrastructure, and the multivariate data surface was converted into a continuous scalar field using linear grid interpolation and surface-weighted Gaussian kernel smoothing methods. Thus, while preserving the directional structure of the bipolar recordings, the relative distribution across the entire head surface was estimated for each metric and converted into color-scaled topographic maps. In the final step, the interpolation mask was constrained to exclude the ear and face regions, and all maps were converted into the final topoplots shown in Figure 2 and Figure 3 using normalized common color scales.

Statistical analyses were performed at the subject level. Two-way repeated measures ANOVA was applied for each patient, with condition (preictal vs. interictal; early preictal vs. late preictal) and channel as within-subject factors. Data entries were structured to include multiple measurements in each cell, and post-hoc tests with Šídák correction were used for multiple comparisons. Parametric assumptions were checked in the analyses. All statistical procedures were performed using GraphPad Prism 10 software, and results were considered significant at $p < 0.05$.

3. Results and Discussion

3.1 Results

Electrophysiological markers between the preictal and interictal periods were evaluated for each bipolar channel both statistically (mean ± SD) and in terms of their spatial distribution. These parameters were extracted for each channel × window. Figure 2 presents bar graphs of channel-based mean values, followed by cortical topographies of the same metrics, illustrating regional change patterns specific to the preictal state.

When comparing preictal and interictal states (Figure 2A), the preictal period in the FT9-FT10 channel was characterized by statistically significantly higher DFA values compared to the interictal period ($p < 0.05$). Topographic maps show that signal self-similarity is generally higher in the preictal period compared to the interictal period, particularly in the frontal regions. When spectral content differences between the two conditions were examined (Figure 2B), the left fronto-central (F3-C3) channel was found to be significantly higher in the preictal period compared to the interictal segment ($p < 0.05$). In the right parieto-temporal (T8-P8) channel, this change reversed direction, and a significant increase was observed in the interictal period compared to the preictal period ($p < 0.05$). When topographic maps were examined, high-frequency activity (yellow/bright areas) in the preictal period formed a distinct focus concentrated in the left fronto-central and midline regions, while in the interictal period, this frontal activity was attenuated and the high MPF focus shifted to the parieto-occipital region of the right hemisphere. This finding is consistent with the interpretation that the frequency distribution underwent a diagonal axis shift from anterior-left to posterior-right during the transition from the preictal to the interictal period. Aperiodic Spectral Slope revealed regional differences between the preictal and interictal periods. Although not statistically significant in almost all channels, interictal spectral slopes showed an increase compared to the preictal period. The FOOOF Algorithm detected that β values in the interictal period were significantly higher ($p < 0.05$) compared to the preictal period in the T7-P7 and P7-T7 channels in the left temporal-parietal region.

Celal Bayar University Journal of Science
Volume 22, Issue 2, 2026, p 284-294
Doi: 10.18466/cbayarfbe.1829844

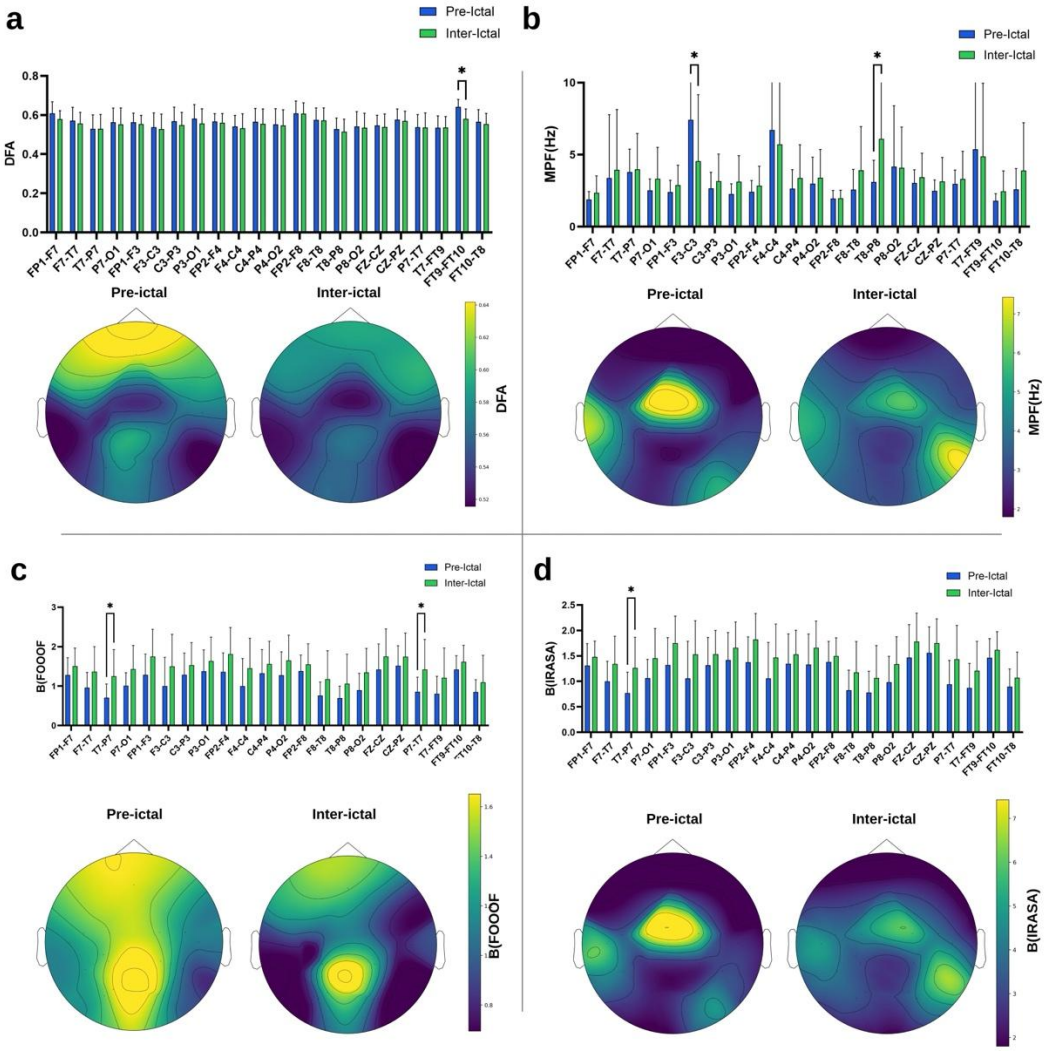

Figure 2. Topographic and statistical comparison of electrophysiological parameters between preictal and interictal periods. Each subpanel represents a different quantitative metric derived from EEG, analyzed via bipolar derivatives and projected onto scalp topographies. (A) DFA-α values calculated from the wideband amplitude envelope, (B) Median Power Frequency (MPF) derived from Welch spectral estimates (0.5–45 Hz, 8-second window, 50% overlap), (C) Aperiodic exponent β estimated by SpecParam (FOOOF; 2–40 Hz, fixed mode), (D) β values obtained using the IRASA method (h = 1.1–1.9, Δh = 0.05).

When examining the topographic distribution, it was observed that high β values in the preictal period exhibited a broad and widespread distribution covering the entire frontal lobe and extending along the central midline to the vertex. In contrast, during the interictal period, this broad frontal activity was attenuated, and the high spectral slope focus shifted to a narrower area limited to the posterior midline (parieto-occipital region) (Figure 2C). Analysis using the IRASA method also showed that the spectral slope in the T7-P7 channel during the interictal period was significantly higher than during the preictal period ($p < 0.05$). During the preictal period, high β activity clustered in a fairly well-defined (isolated) and intense focus in the fronto-central region (around the Fz-Cz electrodes). Upon transition to the interictal period, this central focus completely disappeared and was replaced by a lower-intensity activity localized to the right posterior-temporal region (around T8-P8) (Figure 2D).

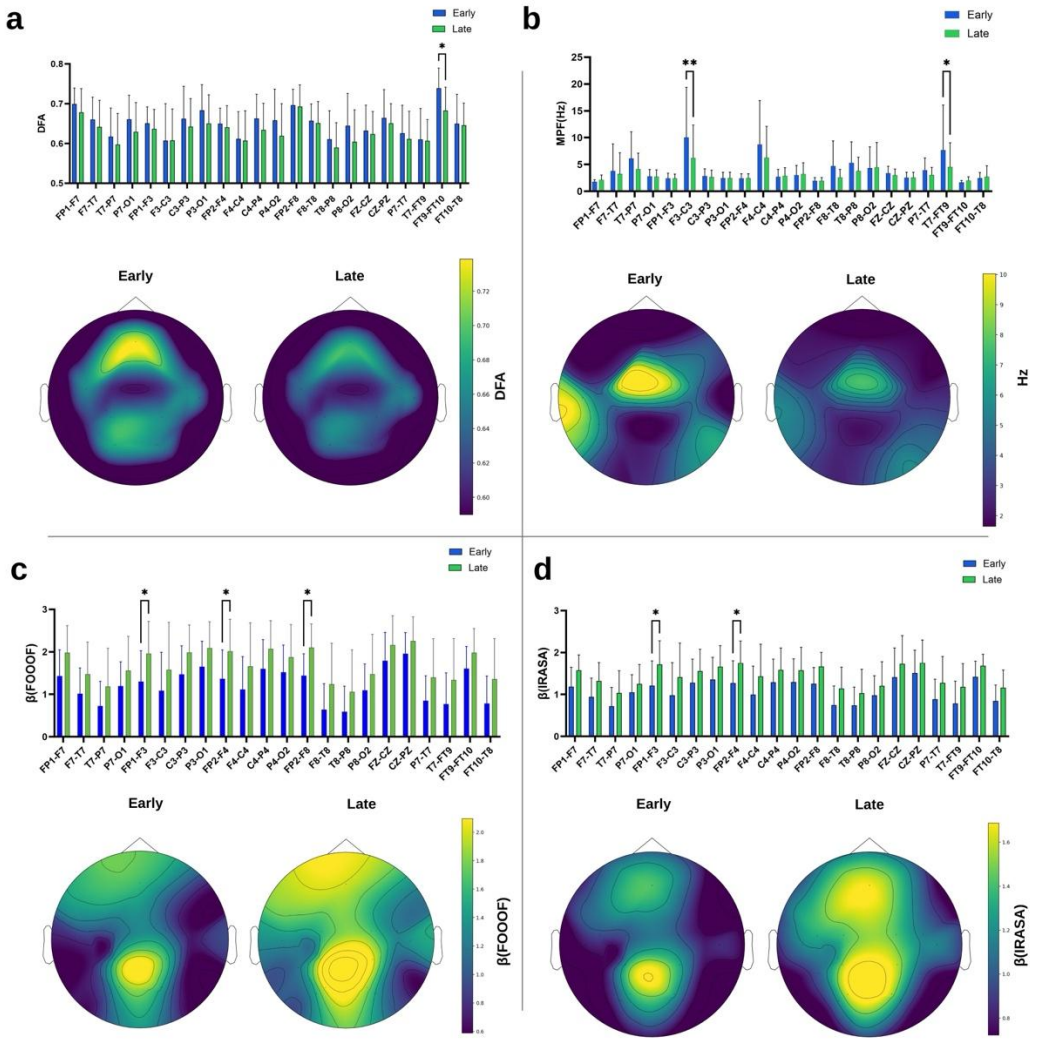

Figure 3. *Comparison of electrophysiological features between the early and late preictal periods.* Each panel represents a different quantitative EEG parameter obtained from bipolar scalp recordings. (A) DFA analysis of wideband amplitude envelopes quantifying long-range temporal correlations; mean values across channels are plotted for early and late preictal periods, with statistically significant differences determined by two-way ANOVA ($p < 0.05$, Šídák correction). (B) Median Power Frequency (MPF, Hz) obtained from Welch spectral estimates (0.5–45 Hz, 8-second window, 50% overlap) reflects spectral shifts in frequency content between cortical regions. (C) The aperiodic exponent β estimated using SpecParam (FOOOF; 2–40 Hz, fixed mode fit) and (D) β derived from the IRASA method ($h = 1.1–1.9$, $\Delta h = 0.05$), both quantify the 1/f spectral slope after separation of aperiodic and oscillatory components (Wen & Liu, Brain Topogr., 2016).

When examining the temporal dynamics within the preictal period (Figure 3A), a statistically significant decrease in DFA scaling exponents was observed in the FT9-FT10 channel as the seizure approached (Late period) compared to the Early period ($p < 0.05$). In topographic maps, the high signal self-similarity concentrated in the frontal region during the early preictal period (yellow/bright areas) underwent a marked attenuation in the late period, giving way to lower correlation values (blue/green areas). A similar attenuation trend was also detected in the MPF analysis (Figure 3B). In the F3-C3 channel, late preictal period values showed a highly significant decrease compared to the early period ($p < 0.01$), while a significant decrease was also detected in the FT9-FT10 channel ($p<0.05$). When examining the topographic maps, an isolated and distinct high-frequency cluster is observed in the left fronto-central region during the early preictal period. However, upon transition to the late period, this left frontal focus is completely dispersed, and frequency values decrease across the entire scalp, indicating slowed activity. According to the FOOOF algorithm results (Figure 3C), β values in the Late period in the FP1-F3, FP2-F4, and FP2-F8 channels in the frontal region showed a significant increase compared to the Early period ($p<0.05$). When examining the topographic distribution, it is seen that in the early period, high spectral slope values are only present as a weak focus in

the posterior midline. In the late period immediately before the seizure, while this posterior focus is preserved, the activity has shifted anteriorly in a severe manner, forming a large and dominant high-slope area (yellow/bright) covering the entire prefrontal and frontal cortex. Consistent with this finding, the IRASA method (Figure 3D) also confirmed that spectral slope significantly steepened in the FP1-F3 and FP2-F4 channels as the seizure approached ($p<0.05$). IRASA topographic maps also show a posterior-anterior spread consistent with FOOOF findings. Activity, which was limited to the parieto-occipital region in the early stage, expanded significantly in the late stage, forming a new and intense focus in the fronto-central regions.

3.2 Discussion

I

This study investigated the spatiotemporal reorganization of scale-independent EEG dynamics during the preictal period in pediatric focal epilepsy, using three complementary metrics: long-range temporal correlations quantified by DFA-α, spectral content indexed by MPF, and the aperiodic background exponent β estimated by both FOOOF/SpecParam and IRASA. The principal findings were as follows. Compared to interictal segments, preictal windows showed increased DFA-α and MPF in fronto-temporal regions, with β values exhibiting a broad frontal distribution. Within the preictal period, the transition from early to late phase was associated with a marked decrease in fronto-temporal DFA-α and MPF, accompanied by a posterior-to-anterior expansion of aperiodic β steepening. These patterns are discussed below in the context of current theoretical frameworks of preictal network dynamics, critical state transitions, and seizure generation. This study uses long-range temporal correlations (DFA-α), median power frequency (MPF), and the aperiodic 1/f exponent β obtained from both parametric (FOOOF/SpecParam) and resampling-based (IRASA) decompositions; to investigate how scale-independent EEG dynamics reorganize in space and time as seizures approach. Preictal segments were characterized by increased DFA-α predominantly in frontal regions and a focal increase in MPF at left fronto-central contacts compared to interictal segments. Additionally, a diagonal shift of the MPF maximum from an anterior-left focus in the preictal period to a right parieto-occipital focus in the interictal period was observed. Approaching seizure onset (late preictal period), a marked decrease in DFA-α and MPF values was observed in fronto-temporal channels. This decrease was accompanied by a steepening of the aperiodic spectral slope. This steepening, located at the posterior midline focus in the early preictal period, spread to a broad prefrontal-frontal area in the late period. This dynamic change was consistently confirmed by both FOOOF and IRASA methods. Taken together, the findings indicate that the preictal process is characterized by a collapse of temporal complexity and spectral slowing in fronto-temporal networks, concurrent with a large-scale reorganization of the aperiodic (1/f) background.

DFA-based long-range temporal correlations (LRTC) measurements are accepted as sensitive descriptors of scale-independent brain dynamics in human magnetoencephalography (MEG) and EEG. Linkenkaer-Hansen et al. demonstrated that alpha and beta band amplitude envelopes exhibit persistent LRTC ($\alpha \approx 0.6–0.9$) across time scales ranging from seconds to minutes, and that these correlations are modulated by behavioral state [7,18]. Subsequent studies using fMRI and EEG have linked changes in scale-independent exponents to deviations from critical network dynamics in consciousness disorders, pharmacological anesthesia, and neuropsychiatric diseases [19]. The current results extend this framework to the preictal period of pediatric intractable epilepsy. Compared to interictal segments, preictal windows showed locally increased DFA-α on fronto-basal contacts (FT9–FT10), and topographic maps generally indicated higher self-similarity over the frontal cortex. This model is consistent with the first approach reporting that fluctuations show greater temporal correlation, as proposed in theoretical studies on critical transitions [4]. In the seizure context, studies using autocorrelation-based indices and variance have defined “critical slowing” as a preictal warning signal and indicated that changes develop over hours or days rather than minutes [6]. Meisel and colleagues (2012) reported that seizures represent a deviation from the system's adaptive, self-organizing criticality (SOC) and a drift toward a pathological attractor. When evaluated alongside the critical slowing down signs observed in long-term recordings [6], the decrease in DFA in our findings is consistent with the preictal network losing its stability by moving away from the optimal critical regime (complexity loss) [20]. With this approach, it can be concluded that the epileptic network may temporarily approach a critical regime and then pass it, while the late preictal period reflects the collapse of the scale-independent temporal structure as the seizure approaches.

DFA was calculated on band-limited Hilbert amplitude envelopes. This methodological choice is consistent with validated fast DFA applications on physiological time series and ensures that the changes reported in α primarily reflect envelope dynamics rather than narrow-band artifacts. The observation that preictal DFA-α decreases are most pronounced in inferior fronto-temporal contacts is consistent with the interpretation that they disrupt long-range dependencies in regions playing a strong role in seizure initiation and propagation within the epileptogenic network, while more posterior regions maintain a relatively stable scale-independent structure.

MPF provided a complementary summary of the oscillatory content. Between the preictal and interictal

periods, MPF increased over left fronto-central contacts during preictal segments and shifted toward the right parieto-occipital cluster during interictal segments, indicating a reorganization of dominant frequencies from pre-left to post-right across all conditions. Within the preictal period, both F3–C3 and FT9–FT10 showed significant MPF decreases from the beginning to the end of the preictal period, and the topography at the beginning of the preictal period exhibited a well-defined high-frequency island over the left fronto-central cortex; this island disappeared as the onset of the seizure approached and was replaced by generally slower activity. Similar spectral slowing phenomena, characterized by a shift of the dominant or median frequency to lower ranges, have been described in various pathological conditions, including neurogenic pain and widespread cortical dysfunction, and are generally interpreted as reflecting alterations in the thalamocortical drive and impaired information processing capacity [21]. In intracranial epilepsy recordings, preictal power changes outside the seizure onset zone frequently manifest as low frequency strengthening and slowing, which can be interpreted as a general reorganization of large-scale networks rather than purely focal activation [22]. The current scalp EEG results support this view. Late preictal MPF decreases in fronto-temporal regions indicate a shift towards slower, more synchronized dynamics in widespread networks involved in seizure generation.

The aperiodic 1/f exponent β has emerged as a physiologically meaningful marker that goes beyond traditional narrow-band power measurements, tracking arousal, cognitive demands, development, and disease states. Donoghue et al. introduced the SpecParam (FOOOF) algorithm to parameterize neural power spectra into periodic and aperiodic components and demonstrated that the aperiodic exponent systematically changes with aging and task engagement [2]. Similarly, Wen and Liu's IRASA method provides a nonparametric estimate of the fractal background by separating fractal and oscillatory components through irregular resampling of the signal [3]. In the current study, both tools were applied to the same data, yielding convergent β models across conditions. Between the preictal and interictal periods, β values tended to be higher in most channels during interictal segments, with significant increases observed in left temporo-parietal leads (T7–P7, P7–T7). Topographically, relatively high β values were observed in a broad frontal region extending along the midline up to the vertex during preictal periods, whereas this frontal high-β area decreased during interictal periods. However, the dominant β focus narrowed to a more restricted parieto-occipital region and right posterior-temporal cluster. In contrast, during the preictal period, β significantly increased in the prefrontal and frontal derivations (FP1–F3, FP2–F4, FP2–F8). Furthermore, the corresponding maps showed a posterior-anterior spread. Early preictal segments exhibited only a weak posterior midline high β focus, while late preictal segments exhibited a broad prefrontal-frontal high β area, and IRASA maps showed a similar change.

Studies have linked the power law exponent of the field potential spectrum to the underlying E/I balance [23]. Within this framework, the late preictal steepening of β over the prefrontal-frontal cortex, consistent with concurrent MPF decreases in the same regions, may reflect a shift toward an E/I configuration that supports low-frequency synchronization and reduces asynchronous high-frequency activity [11,24]. The generally higher β values exhibited by interictal segments, particularly over the posterior cortex, suggest that the interictal periods of epileptic brains in the CHB-MIT cohort were spent predominantly in a relatively inhibited, dominated by slow activity, and that early preictal dynamics include partial flattening of the spectrum in specific regions such as the left frontal cortex prior to the final pre-seizure steepening. This non-monotonic trajectory emphasizes that aperiodic exponents should be interpreted in relation to both LRTC and oscillation measurements, not in isolation. Another approach to these results can be based on neural hypersynchronization. Increased β values in the late preictal period may reflect a transition towards hypersynchrony with spectral slowing rather than synaptic suppression [11,24]. As the seizure onset approaches, the loss of asynchronous high-frequency complexity and the emergence of slow, high-amplitude rhythmic activities may lead to a steeper power spectral density [24–26]. This approach is also consistent with the “critical slowing down” phenomenon observed in our MPF results.

Common patterns between DFA-α, MPF, and β support a spatiotemporal narrative in which epileptogenic networks reorganize along both anterior-posterior and left-right axes as seizures approach [27]. In the early preictal period, the frontal cortex exhibits a broad distribution of elevated DFA-α and MPF alongside moderately increased β, a pattern consistent with a network operating near a critical point that supports rich temporal structure and complex dynamics [7,10]. This pre-seizure preparatory state characterized by maintained long-range correlations and relatively flat aperiodic spectra is unstable. As seizure onset approaches, it gives way to the coordinated collapse of temporal complexity and spectral slowing described above, which we interpret as the signature of the preictal network crossing its critical threshold. As seizure time decreases, LRTC and MPF collapse in the inferior fronto-temporal areas [6], β dramatically steepens over the prefrontal and frontal cortex, and the initial posterior high β focus expands anteriorly [2]. Interictal segments, on the other hand, are characterized by a posterior shift of the MPF maximum toward the right parieto-occipital regions and a significant weakening of frontal β activity, with more localized posterior high β areas [3].

From a seizure prediction perspective, the adopted temporal framework (SPH = 5 minutes, SOP = 30 minutes, preictal = −35 to −5 minutes) is consistent with recent recommendations emphasizing clear definitions of seizure prediction horizon and formation time when reporting algorithm performance. Seizure prediction studies increasingly evaluate models in terms of sensitivity, false prediction rate per hour, and warning time, defining SPH/SOP pairs to avoid trivial solutions with fixed high-risk states [28,29]. While this study does not propose a prediction classifier, it identifies preictal windows where scale-independent metrics systematically change at the network level. Relatively stable increases in DFA-α and MPF are observed in the left frontal regions during the early preictal period, while rapid decreases in DFA-α and MPF and steepening of β in the frontal cortex dominate during the late preictal period. This suggests that early preictal intervals may be a more stable segment for feature extraction in prediction algorithms. The nature of late preictal dynamics, however, may be more variable and therefore more suitable for short-term warning systems rather than long-term risk prediction.

4. Conclusion

This study indicates that the preictal period in pediatric focal epilepsy may not be a homogeneous process but rather is characterized by a distinct spatiotemporal reorganization in scale-free network dynamics. Our findings may reflect that the path to seizure begins with a “preparation” phase (early-preictal) marked by increased long-range correlations in frontal regions, but as seizure onset approaches, this structure gives way to a sudden complexity collapse and spectral slowing. In this process, the steepening of the aperiodic (1/f) spectral slope spreading from posterior to anterior indicates a global collapse in the balance of synchronization and inhibition as epileptic networks approach a critical threshold. In summary, the combined use of fractal (DFA) and aperiodic (1/f) metrics provides a multidimensional and physiologically grounded new framework for monitoring the changing stability states of the preictal brain.

The findings of this study should be interpreted considering several limitations. First, the analyses are restricted to the CHB-MIT Pediatric Scalp EEG Database, which contains recordings from pediatric patients with intractable focal epilepsy. The absence of detailed clinical information on seizure type, semiology, and etiology, combined with the retrospective design, limits the ability to disentangle patient-specific from condition-specific effects and constrains the generalizability of the observed spatiotemporal patterns to adult cohorts or other epilepsy syndromes. Second, the dataset exhibits a notably unbalanced sex distribution (5 males, 17 females) and a wide pediatric age range (1.5–22 years). Age-related differences in cortical maturation and myelination across this range may differentially affect aperiodic slope estimates and DFA scaling exponents, and the female-dominant composition may not be representative of the broader epileptic population. Future studies should validate these findings in demographically balanced cohorts. Third, data were acquired using scalp bipolar montage recordings. This limits spatial resolution and reduces sensitivity to deep or mesial sources. Furthermore, the inherent spatial high-pass filtering of bipolar derivations may systematically reduce absolute aperiodic slope estimates relative to referential montages; consequently, absolute β values should be interpreted with caution, while relative between-condition comparisons remain valid. Fourth, the FOOOF parameterization was applied in 'fixed' mode without a knee parameter, which assumes a purely linear log-log relationship across the fitted frequency range. In pediatric EEG, curvature at low frequencies may lead to a slight overestimation of the aperiodic slope. The convergent results obtained with the model-independent IRASA method mitigate this concern but do not fully eliminate it. Fifth, this study provides a retrospective characterization of preictal dynamics and does not include an explicit machine learning classifier or prospective seizure prediction model; ROC-AUC performance metrics are therefore not available. Finally, the proposed mechanistic links between aperiodic steepening and changes in excitation/inhibition balance have not been directly validated in this dataset. Future studies should combine the scale-free features defined here with multi-channel connectivity analyses and neural mass model simulations, and should validate findings in large, heterogeneous cohorts with intracranial recordings

Acknowledgement

The author gratefully acknowledges the investigators at Boston Children's Hospital and the Massachusetts Institute of Technology (MIT) for collecting the data and making the CHB-MIT Scalp EEG Database publicly available via PhysioNet. The author also thanks the open-source community for developing the Python tools (MNE, SciPy, FOOOF) used in this research.

Author’s Contributions

The author confirms sole responsibility for study conception and design, data analysis and interpretation, and manuscript preparation.

Ethics

This study did not require additional Ethics Committee Approval as it involves a secondary analysis of a completely anonymized, publicly available dataset (CHB-MIT Scalp EEG Database, PhysioNet; https://physionet.org/content/chbmit/1.0.0). The original data collection was approved by the Boston Children's

Hospital and Massachusetts Institute of Technology (MIT) Institutional Review Boards and conducted in accordance with the Declaration of Helsinki.

References

[1]. Mormann F, Andrzejak RG, Elger CE, Lehnertz K. Seizure prediction: the long and winding road. Brain 2007;130:314–33. https://doi.org/10.1093/BRAIN/AWL241.

[2]. Donoghue T, Haller M, Peterson EJ, Varma P, Sebastian P, Gao R, et al. Parameterizing neural power spectra into periodic and aperiodic components. Nat Neurosci 2020;23:1655–65. https://doi.org/10.1038/S41593-020-00744-X.

[3]. Wen H, Liu Z. Separating Fractal and Oscillatory Components in the Power Spectrum of Neurophysiological Signal. Brain Topogr 2016;29:13–26. https://doi.org/10.1007/S10548-015-0448-0.

[4]. He BJ, Zempel JM, Snyder AZ, Raichle ME. The temporal structures and functional significance of scale-free brain activity. Neuron 2010;66:353. https://doi.org/10.1016/J.NEURON.2010.04.020.

[5]. Gadhoumi K, Gotman J, Lina JM. Scale Invariance Properties of Intracerebral EEG Improve Seizure Prediction in Mesial Temporal Lobe Epilepsy 2015. https://doi.org/10.1371/journal.pone.0121182.

[6]. Maturana MI, Meisel C, Dell K, Karoly PJ, D'Souza W, Grayden DB, et al. Critical slowing down as a biomarker for seizure susceptibility. Nature Communications 2020 11:1 2020;11:2172-. https://doi.org/10.1038/s41467-020-15908-3.

[7]. Linkenkaer-Hansen K, Nikouline V V., Palva JM, Ilmoniemi RJ. Long-range temporal correlations and scaling behavior in human brain oscillations. J Neurosci 2001;21:1370–7. https://doi.org/10.1523/JNEUROSCI.21-04-01370.2001.

[8]. Castiglioni P, Faini A. A Fast DFA Algorithm for Multifractal Multiscale Analysis of Physiological Time Series. Front Physiol 2019;10. https://doi.org/10.3389/fphys.2019.00115.

[9]. Peng CK, Havlin S, Stanley HE, Goldberger AL. Quantification of scaling exponents and crossover phenomena in nonstationary heartbeat time series. Chaos. 1995;5(1):82-7. doi: 10.1063/1.166141. PMID: 11538314.

[10]. Meisel C, Klaus A, Kuehn C, Plenz D. Critical slowing down governs the transition to neuron spiking. PLoS Comput Biol 2015;11. https://doi.org/10.1371/JOURNAL.PCBI.1004097.

[11]. Westin K, Cooray G, Beniczky S, Lundqvist D. Interictal epileptiform discharges in focal epilepsy are preceded by increase in low-frequency oscillations 2022. https://doi.org/10.1016/j.clinph.2022.02.003.

[12]. Ibarra Chaoul A, Siegel M. Cortical correlation structure of aperiodic neuronal population activity. Neuroimage 2021;245:118672. https://doi.org/10.1016/J.NEUROIMAGE.2021.118672.

[13]. Goldberger AL, Amaral LA, Glass L, Hausdorff JM, Ivanov PC, Mark RG, et al. PhysioBank, PhysioToolkit, and PhysioNet: components of a new research resource for complex physiologic signals. Circulation 2000;101. https://doi.org/10.1161/01.cir.101.23.e215.

[14]. Shoeb AH. Application of Machine Learning to Epileptic Seizure Onset Detection and Treatment MASS NSl OF TECHNOLOGY. 2009.

[15]. Lendner JD, Helfrich RF, Mander BA, Romundstad L, Lin JJ, Walker MP, et al. An electrophysiological marker of arousal level in humans. Elife 2020;9:e55092. https://doi.org/10.7554/ELIFE.55092.

[16]. Gramfort A, Luessi M, Larson E, Engemann DA, Strohmeier D, Brodbeck C, et al. MNE software for processing MEG and EEG data. Neuroimage 2014;86:446–60. https://doi.org/10.1016/J.NEUROIMAGE.2013.10.027.

[17]. Virtanen P, Gommers R, Oliphant TE, Haberland M, Reddy T, Cournapeau D, et al. SciPy 1.0: fundamental algorithms for scientific computing in Python. Nature Methods 2020 17:3 2020;17:261–72. https://doi.org/10.1038/s41592-019-0686-2.

[18]. Tagliazucchi E, Von Wegner F, Morzelewski A, Brodbeck V, Jahnke K, Laufs H. Breakdown of long-range temporal dependence in default mode and attention networks during deep sleep. Proc Natl Acad Sci U S A 2013;110:15419–24. https://doi.org/10.1073/PNAS.1312848110

[19]. He BJ. Scale-Free Properties of the Functional Magnetic Resonance Imaging Signal during Rest and Task. The Journal of Neuroscience 2011;31:13786. https://doi.org/10.1523/JNEUROSCI.2111-11.2011.

[20]. Meisel C, Kuehn C. Scaling Effects and Spatio-Temporal Multilevel Dynamics in Epileptic Seizures. PLoS One 2012;7:e30371. https://doi.org/10.1371/JOURNAL.PONE.0030371.

[21]. Sarnthein J, Stern J, Aufenberg C, Rousson V, Jeanmonod D. Increased EEG power and slowed dominant frequency in patients with neurogenic pain. Brain 2006;129:55–64. https://doi.org/10.1093/BRAIN/AWH631.

[22]. Naftulin JS, Ahmed OJ, Piantoni G, Eichenlaub JB, Martinet LE, Kramer MA, et al. Ictal and Preictal Power Changes Outside of the Seizure Focus Correlate with Seizure Generalization. Epilepsia 2018;59:1398. https://doi.org/10.1111/EPI.14449.

[23]. Gao Y, Chen X, Liu A, Liang D, Wu L, Qian R, et al. Pediatric Seizure Prediction in Scalp EEG Using a Multi-Scale Neural Network With Dilated Convolutions. IEEE J Transl Eng Health Med 2022;10:4900209. https://doi.org/10.1109/JTEHM.2022.3144037.

[24]. Li F, Liang Y, Zhang L, Yi C, Liao Y, Jiang Y, et al. Transition of brain networks from an interictal to a preictal state preceding a seizure revealed by scalp EEG network analysis. Cogn Neurodyn 2019;13:175–81. https://doi.org/10.1007/S11571-018-09517-6.

[25]. Alvarado-Rojas C, Valderrama M, Fouad-Ahmed A, Feldwisch-Drentrup H, Ihle M, Teixeira CA, et al. Slow modulations of high-frequency activity (40-140â ...Hz) discriminate preictal changes in human focal epilepsy. Sci Rep 2014;4. https://doi.org/10.1038/SREP04545.

[26]. Jiruska P, Csicsvari J, Powell AD, Fox JE, Chang WC, Vreugdenhil M, et al. High-frequency network activity, global increase in neuronal activity, and synchrony expansion precede epileptic seizures in vitro. Journal of Neuroscience 2010; 30:5690–701. https://doi.org/10.1523/JNEUROSCI.0535-10.2010.

[27]. Kramer MA, Cash SS. Epilepsy as a disorder of cortical network organization. Neuroscientist 2012;18:360–72. https://doi.org/10.1177/1073858411422754.

[28]. Ren Z, Han X, Wang B. The performance evaluation of the state-of-the-art EEG-based seizure prediction models. Front Neurol 2022;13:1016224. https://doi.org/10.3389/FNEUR.2022.1016224/FULL.

[29]. Nazari J, Motie Nasrabadi A, Menhaj MB, Raiesdana S. Epilepsy seizure prediction with few-shot learning method n.d. https://doi.org/10.1186/s40708-022-00170-8.